electronics

MDPI

Article

A New Design Method for Class-E Power Amplifiers Using Artificial Intelligence Modeling for Wireless Power Transfer Applications

Salah I. Yahya [1,2], Ban M. Alameri [3], Mohammad (Behdad) Jamshidi [4,5], Saeed Roshani [6], Muhammad Akmal Chaudhary [7], Gerald K. Ijemaru [8,*], Yaqeen Sabah Mezaal [9] and Sobhan Roshani [6,*]

1 Department of Communication and Computer Engineering, Cihan University-Erbil, Erbil 44001, Iraq
2 Department of Software Engineering, Faculty of Engineering, Koya University, Koya KOY45, Iraq
3 Department of Electrical Engineering, Faculty of Engineering, Mustansiriyah University, Baghdad 10053, Iraq
4 Regional Innovation Centre for Electrical engineering (RICE), University of West Bohemia in Pilsen, 30100 Pilsen, Czech Republic
5 Department of Power Electronics and Machines (KEV) University of West Bohemia Pilsen, 30100 Pilsen, Czech Republic
6 Department of Electrical Engineering, Kermanshah Branch, Islamic Azad University, Kermanshah 6718997551, Iran
7 College of Engineering and Information Technology, Ajman University, Ajman P.O. Box 346, United Arab Emirates
8 School of Science, Technology and Engineering, Moreton Bay Campus, University of the Sunshine Coast, Moreton Parade, Petrie, QLD 4502, Australia
9 Medical Instrumentation Engineering Department, Al-Esraa University College, Baghdad 10071, Iraq
* Correspondence: gerald.ijemaru@research.usc.edu.au (G.K.I.); s.roshani@aut.ac.ir (S.R.)

check for updates

Citation: Yahya, S.I.; Alameri, B.M.; Jamshidi, M.; Roshani, S.; Chaudhary, M.A.; Ijemaru, G.K.; Mezaal, Y.S.; Roshani, S. A New Design Method for Class-E Power Amplifiers Using Artificial Intelligence Modeling for Wireless Power Transfer Applications. *Electronics* **2022**, *11*, 3608. https://doi.org/10.3390/electronics11213608

Academic Editor: Nicu Bizon

Received: 7 October 2022
Accepted: 2 November 2022
Published: 4 November 2022

Abstract: This paper presents a new approach to simplify the design of class-E power amplifier (PA) using hybrid artificial neural-optimization network modeling. The class-E PA is designed for wireless power transfer (WPT) applications to be used in biomedical or internet of things (IoT) devices. Artificial neural network (ANN) models are combined with optimization algorithms to support the design of the class-E PA. In several amplifier circuits, the closed form equations cannot be extracted. Hence, the complicated numerical calculations are needed to find the circuit elements values and then to design the amplifier. Therefore, for the first time, ANN modeling is proposed in this paper to predict the values of the circuit elements without using the complex equations. In comparison with the other similar models, high accuracy has been obtained for the proposed model with mean absolute errors (MAEs) of 0.0110 and 0.0099, for train and test results. Moreover, root mean square errors (RMSEs) of 0.0163 and 0.0124 have been achieved for train and test results for the proposed model. Moreover, the best and the worst-case related errors of 0.001 and 0.168 have been obtained, respectively, for the both design examples at different frequencies, which shows high accuracy of the proposed ANN design method. Finally, a design of class-E PA is presented using the circuit elements values that, first, extracted by the analyses, and second, predicted by ANN. The calculated drain efficiencies for the designed class-E amplifiers have been obtained equal to 95.5% and 91.2% by using analyses data and predicted data by proposed ANN, respectively. The comparison between the real and predicted values shows a good agreement.

Keywords: artificial neural network; class-E amplifier; genetic algorithm; imperialist competitive; particle swarm optimization

1. Introduction

Wireless power transfer (WPT) means transmission of electrical energy without wires or any physical links, which was first introduced by Nicola Tesla in 1914 [1]. Recently, the wireless transmission of energy has become more interesting and popular in several applications, such as biomedical science [2], internet of things (IoT) [3], electrical vehicles [4],

and sensor networks [5]. The WPT can be generally divided in two categories of far-field and near-field techniques, where the near-field technique is studied in this paper. The near-field WPT utilizes inductive coupling effect to wirelessly transfer energy [6]. The usage of battery is undesirable in implantable biomedical devices due to the limitation of the energy storage capacity and the need for recharging the battery. Moreover, the risk of possible infection due to the battery inside implantable biomedical devices urges high demands for WPT in biomedical applications [7]. The power amplifier (PA) component plays an important role in the biomedical devices [2]. Among the PAs are the switching amplifiers, especially class-E type, which have a high efficiency and are desirable in biomedical applications [8–12]. The schematic of wireless power transfer with class-E PA using inductive coupling technique is illustrated in Figure 1.

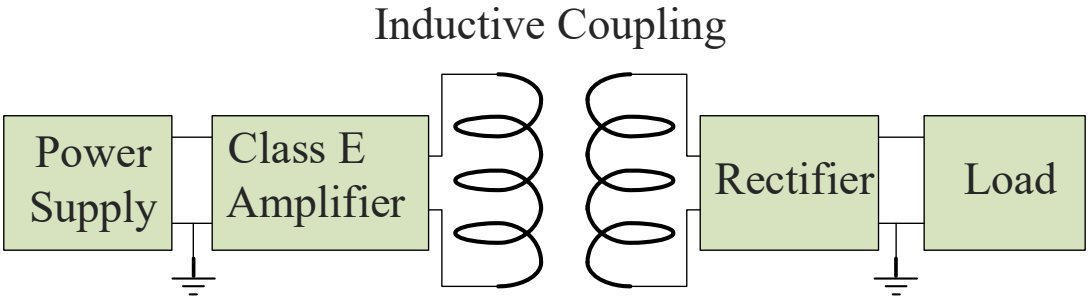

Figure 1. Schematic of the inductive coupling WPT with class-E amplifier.

The class-E amplifier structure was introduced in 1975 by Sokal [13]. In the class-E type amplifiers, the transistor works as a switch. Additionally, the switching pattern shapes the current and voltage of the transistor. The ideal efficiency can be achieved for class-E PA in theory. There are two main conditions in class-E PA, which guarantee a high operation efficiency [14]. These conditions are zero voltage switching (ZVS) and zero derivative switching (ZDS). There are several topologies for class-E PAs, such as shunt capacitance [15], sub-nominal conditions [16] and inverse class-E [17]. Class-E PAs are widely used in several applications, such as biomedical [18], DC-DC power converter [19], rectifiers [20], RF heating [21], and wireless power transfer (WPT) [22,23] applications. The amplifiers can be realized in the forms of discrete [8–12] and integrated circuits (ICs) [24,25]. Additionally, photonic crystal fibers, which are used to achieve higher speeds and higher frequencies [26–29], can be used for amplifiers design [30,31].

Extracting the equations of the class-E PA circuit is an important step in the design process of the amplifier. The circuit elements can be calculated using the equations established. Some researchers have studied the effects of parasitic and nonlinear elements in the PA circuit, which result in complicated equations [8,9,32]. Subsequently, an artificial neural network (ANN) model can be useful to help find the circuit elements of the amplifier. Recently, ANN techniques have been used to solve several engineering and electronics problems [33–36]. ANN have also been used to model microwave circuits behavior [37–40]. A class-F amplifier at 1.8 GHz has been designed and modeled in [37], where the radial basis function (RBF) type of neural network has been utilized to model the amplifier circuit. A PSO algorithm is used in [41] to improve the efficiency and frequency of the WPT system. A back propagation neural network and a Simulink MATLAB model are used in [42] to emulate the distance, gape, and noise effects on a WPT system, which can estimate the voltage of the receiver coil as a function of time. System modeling and ANN are used in [43] to design a WPT system identification method for predicting load resistance and mutual inductance and parameters. A review was performed in [44], in which several ANN and optimization algorithms for WPT system have been highlighted. However, [44] used ANN to optimize some parameters in the WPT, such as maximizing the power transfer or reducing the frequency splitting.

In all of the mentioned works in the literature, neural networks or optimization algorithms have been used for optimizing the WPT output parameters or for output parameters prediction. However, in the proposed work, ANNs with optimization algorithms have been utilized to predict the circuit elements values with desired output parameters.

In this paper, a multilayer perceptron (MLP) network, which has high precision for modeling and prediction, is selected as the main neural network structure of the model. The conventional MLP networks use back propagation algorithm (BPA) to modify the weights of each layer of the MLP. Additionally, most of the conventional ANNs use the back propagation algorithm to train the neural network. However, the back propagation algorithm has some defects, such as getting into local minimum and slow convergence [45]. Recently, popular optimization algorithms have been used in some approaches for optimizing the weights and biases of the neural networks to overcome the back propagation algorithm disadvantages and to have a more accurate design and model [46].

In this work, a hybrid ANN and optimization model is proposed, which can be used to design the class-E PA for WPT applications. The circuit elements of the amplifier can be predicted by using the presented model, considering the desired output parameters. The imperialist competitive algorithm (ICA), genetic algorithm (GA), and particle swarm optimization (PSO) algorithm are used to train the weights and bias of the neural network instead of the back propagation algorithm.

2. Class-E PA Circuit

The considered circuit for designing the class-E PA is illustrated in Figure 2. As can be seen, the transistor acts as a switch in this circuit, where the internal capacitors of the transistor are considered. The IRF510 MOSFET transistor with 80 pF shunt capacitor is selected for this considered circuit. The ideal switching amplifiers can achieve ideal efficiency, theoretically. However, in practice, the parasitic resistors and capacitors of the circuit cause the efficiency to be less than 100%. Accordingly, the structure of the switching amplifier is an important element to obtain high efficiency, and the shunt capacitor class-E PA is one of the most desirable circuits that can achieve high efficiency in several applications.

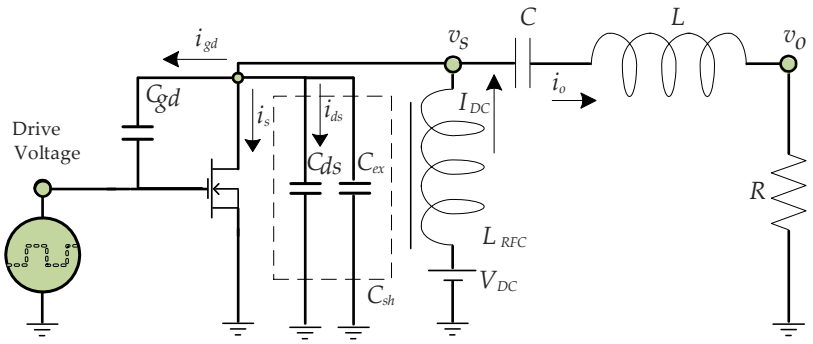

Figure 2. The considered circuit to design the Class-E PA.

The parameter values of operating frequency (f), DC supply voltage (V_{DC}), resonant circuit quality factor (Q), and output power (P_o) are important parameters, which should be specified at the first step of designing the class-E PA. At the next step, based on these parameter values, the circuit elements, such as shunt capacitor (C_{sh}), series inductance (L), series capacitor (C), load resistance (R), and switch voltage (v_s), should be calculated.

The closed form equations can be written for the selected schematic of amplifier according to [14], which is complicated. However, if the MOSFET parasitic elements or the other circuit parasitic elements are considered, it will be impossible to extract the closed form equations and calculate the circuit elements values. The equations for class-E amplifier

circuit shown in Figure 2 can be written according to [8]. Using a KCL for the switch voltage (v_s) node, Equation (1) can be defined as:

$$I_{DC} = i_{ds} + i_{gd} + i_s + i_o \tag{1}$$

where the currents are defined in Figure 2. Because of the high value of Q assumption, the output current can be considered a pure sinusoidal wave.

$$i_o(\theta) = I_m \sin(\theta + \varphi) \tag{2}$$

In Equation (2), I_m is the amplitude of sinusoidal output current, φ is the phase shift between source voltage and the output current, and $\theta = \omega t$ represents the angular time. Practically, the currents of drain to source (i_{ds}) and gate to drain (*culleycriptgd*) capacitors should be considered according to nonlinear capacitors consideration. Therefore, Equation (1) could be written as:

$$I_{DC} = \omega(C_{j01}(1 + v_s/V_{bi1})^{-m1} + C_{j02}(1 + v_{gd}/V_{bi2})^{-m2})\frac{dv_s}{d\theta} + I_m \sin(\theta + \varphi). \tag{3}$$

where C_{j01} and C_{j02} are initial drain-to-source and initial gate-to-drain capacitors. Additionally, V_{bi1} and V_{bi2} are built-in potentials related to drain-to-source and gate-to-drain capacitors. The describing equation for the switch voltage (v_s) can be obtained by integrating from Equation (3), which is written as follows:

$$\begin{aligned} &\frac{\omega RC_{j01}}{\frac{V_{DC}}{V_{bi1}}(1-m_1)}\left(1 + \frac{v_s}{V_{DC}} \times \frac{V_{DC}}{V_{bi1}}\right)^{1-m_1} + \frac{\omega RC_{j02}}{\frac{V_{DC}}{V_{bi2}}(1-m_2)}\left(1 + \frac{v_s}{V_{DC}} \times \frac{V_{DC}}{V_{bi2}}\right)^{1-m2} \\ &- \frac{RI_{DC}\theta}{V_{DC}} - \frac{RI_m}{V_{DC}}(\cos(\theta + \varphi) - \cos(\varphi)) - \frac{\omega RC_{j01}}{\frac{V_{DC}}{V_{bi1}}(1-m_1)} - \frac{\omega RC_{j02}}{\frac{V_{DC}}{V_{bi2}}(1-m_2)} = 0 \quad , \end{aligned} \tag{4}$$

In Equation (4), m_i is the grading coefficient; this parameter corresponds to nonlinear drain-to-source and nonlinear gate-to-drain capacitors. Equation (4) should be solved using initial conditions to extract the waveform equations. This equation has not closed form solution. However, in this paper, the effect of C_{ex} is considered and all of the capacitors are assumed linear to analyze the class-E PA. Therefore, in this case, the switch voltage waveform is simplified as Equation (5), according to [14]. Additionally, the other circuit parameters could be obtained based on the switch voltage waveform, which are fully described in [14].

$$v_s = \frac{I_{DC}}{\omega\, C_{sh}}\left(\omega\, t - \frac{3\pi}{2} - \frac{\pi}{2}\cos\omega\, t - \sin\cos\omega\, t\right) \tag{5}$$

The ANN is a good solution to design any amplifier circuit according to the selected design parameters. The procedure of applying neural network and optimization algorithms to model the presented circuits is described in the next section.

3. Neural Network Modeling

In this section, the process of class-E PA modeling using neural network and optimization algorithms are discussed. To design a class-E PA, the values of V_{DC}, P_o, f, and Q should be defined first, which are considered as the ANN input parameters. Then, the circuit elements can be calculated, based on the extracted equations (1)-(5) and also basic switching amplifier equations in [14]. Hence, the circuit elements of R, C, L, C_{sh}, v_o and v_s are assumed as the ANN output parameters. The proposed ANN model for designing of the class-E PA is depicted in Figure 3.

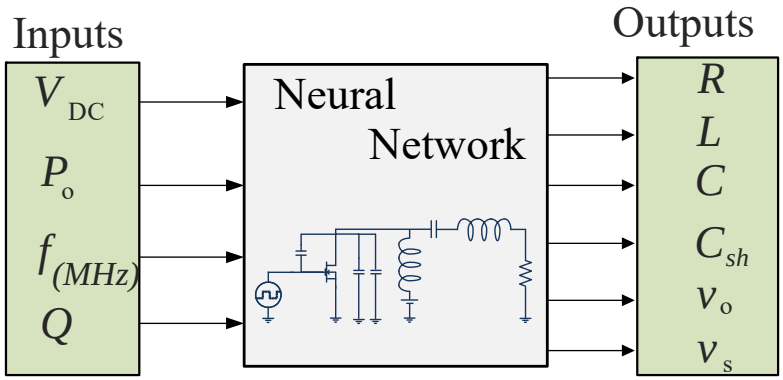

Figure 3. The proposed ANN model for modeling of the class-E amplifier.

3.1. Proposed Model Implementation

Recently, several different types of ANN have been presented, which could be utilized to implement the proposed model. An MLP is a feed forward type of ANN, which has high precision for modeling and prediction applications. The MLP network has three layers: input, hidden, and output layers. There is a number of neurons in each layer with an activation function, and each neuron is connected to neurons in the subsequent layer with weighted connections. The weight values can be calculated during the training process. The proposed structure of the MLP network is selected according to the presented model, which is illustrated in Figure 4.

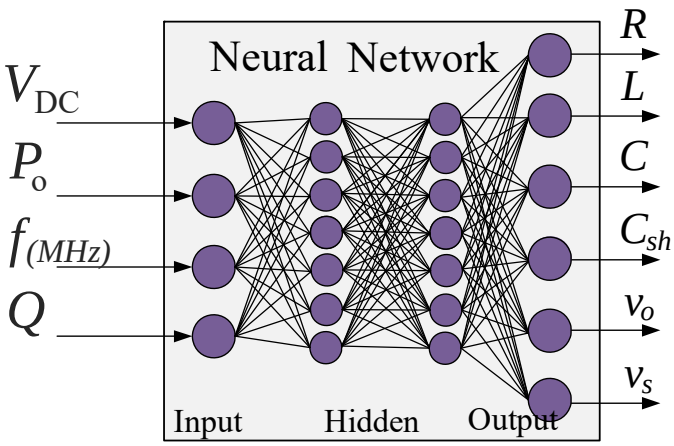

Figure 4. Proposed MLP architecture.

The optimization algorithms are utilized to train the weights and bias of the neural network instead of back propagation algorithm. The optimization methods of ICA, GA, and PSO are used to train the presented network. In other words, these optimization algorithms are used to find the best bias and weights values for the proposed MLP network structure. Therefore, the proposed MLP network structure which uses the optimization algorithms is called the hybrid ANN-optimization algorithm. The procedure of applying the optimization algorithms to the presented ANN model can be illustrated in a flow diagram, which is shown in Figure 5, where MAE is the mean absolute error and RMSE is the root mean squared error. The class-E PA with the presented circuit is analyzed and the circuit elements are extracted using MATLAB software. The presented amplifier is analyzed 100 times with different input parameters to form the dataset for training and testing process of the presented network. Finally, the amplifiers with predicted circuit elements and real circuit elements are simulated and compared using PSpice software.

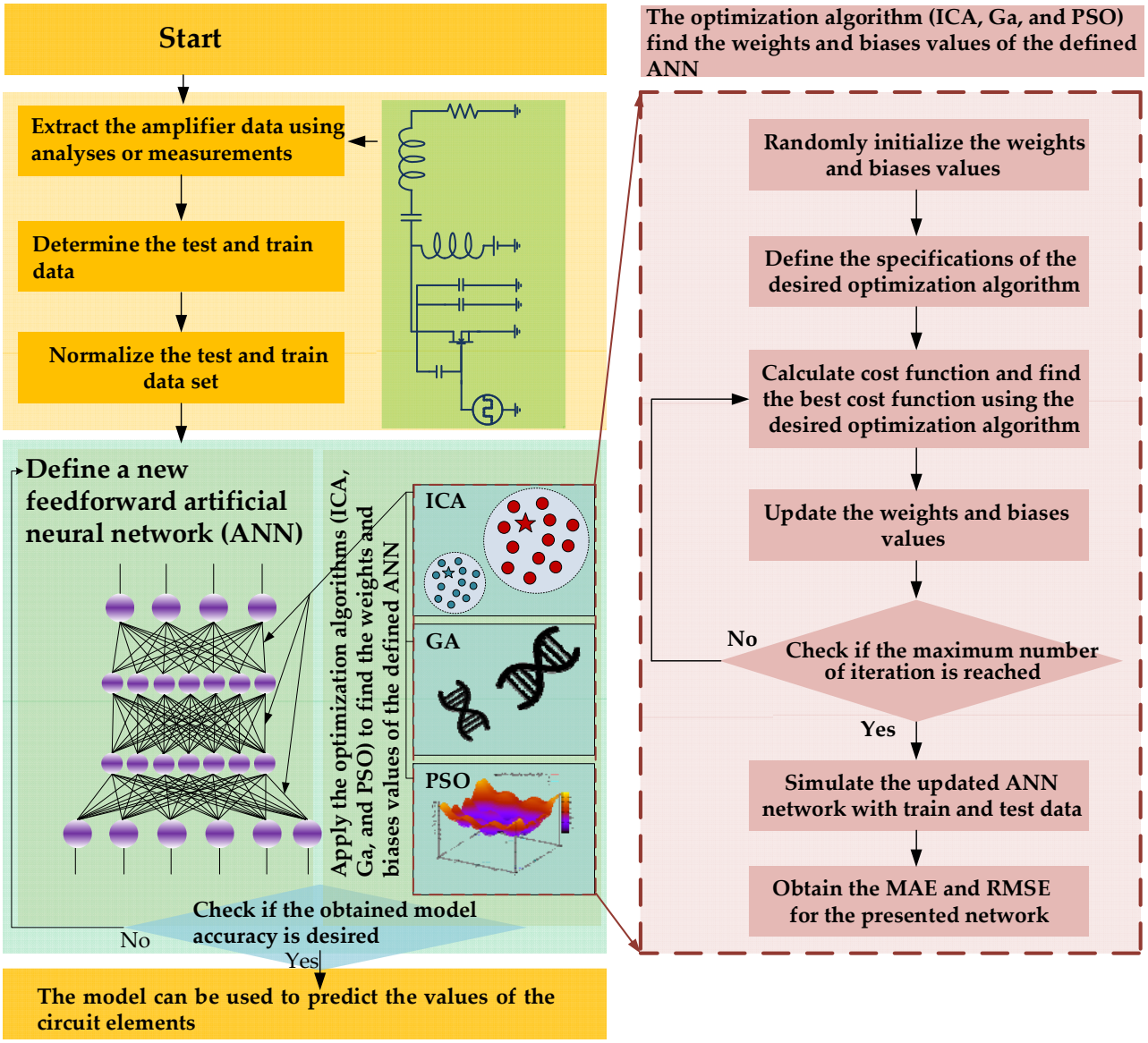

Figure 5. Flow diagram of the presented ANN-optimization algorithm model.

The complexity of the presented feedforward neural network can be defined based on the total number of weights and biases of the network structure. The total number of wights and biases parameters in the feedforward network should be optimized by the applied optimization algorithm. Since a single presented model is used as the ANN model, therefore, three optimization algorithms should optimize same number of parameters. For the presented structure, there are 4 input neurons and 7 neurons in the hidden layers; therefore, there are 28 weight parameters in the input layer and 49 weight parameters in the hidden layers. Additionally, there are 7 biases for each hidden layer containing 7 neurons. Moreover, there are 42 weight parameters and 6 biases for the output layer. Hence, a total number of 139 parameters should be optimized by the applied optimization algorithms.

3.2. Initial Evaluation of the Hybrid ANN-Optimization Algorithms

The utilized optimization algorithms are summarized at the followings. The number of iterations is considered as 100 in the proposed initial networks to save the time in the modeling process for initial evaluation of the proposed algorithms. The specifications of three optimization algorithms, ICA, GA, and PSO algorithms, for initial modeling of the amplifier are listed in Tables 1–3, respectively. After finding the best optimization algorithm

to train the weights and bias of the neural network, the number of 1000 iterations will be selected for the final evaluation of the presented algorithm. In all of the presented algorithms, 80% of the total dataset is applied for training process and the remainder is applied for the test process of the presented model in each network.

3.2.1. MLP-ICA Neural Optimization Network

ICA optimization algorithm has been recently introduced, which can be used for several optimization applications [47]. Similar to PSO and GA, the ICA uses the evolutionary method to obtain the best solution [46]. Among the meta-heuristic algorithms, ICA is one of the most effective algorithms to find the best solution for different problems. This algorithm is inspired from the sociopolitical evolution of humans [48]. Parameters of the ICA algorithm, applied in the presented ANN network, are 500 initial countries, 30 initial imperialists, and 100 iterations. The specifications of the ICA algorithm for initial modeling of the amplifier are listed in Table 1. As mentioned, the low number of iterations is selected according to initial evaluation. The number of initial countries in the ICA algorithms is similar to the initial population in PSO and GA algorithms, while the number of initial imperialists in the ICA is selected based on the [47]. The obtained errors of the proposed ANN-ICA model are given in Table 4. As seen in Table 4, the output circuit element values of the presented ANN-ICA model are close to the real values.

Table 1. The specifications of the ICA algorithm for initial modeling of the amplifier.

Neural network	MLP
Training Algorithm	ICA
Input Layer Neurons	4
Hidden Layer Neurons	7-7
Output Layer Neurons	6
Number of Iterations or Generations	100
Number of Countries	500
Number of Initial Imperialists	30
Activation Function	tansig

3.2.2. MLP-Genetic Neural Optimization Network

GA is inspired from biological genetic evolution process, which has been used in several optimization engineering problems [49–51]. In the GA, chromosomes represent the information. According to the considered fitness function, the best chromosome will be chosen in the population [52]. A set of solutions, named population will be optimized by genetic algorithm. Parameters of the GA algorithm, applied in the presented ANN network, are a population size of 500 and 100 generations. The specifications of the GA algorithm for initial modeling of the amplifier are listed in Table 2. Additionally, the obtained MAE and the RMSE values of the proposed ANN-GA model are shown in Table 4, which show acceptable results.

Table 2. The specifications of the GA algorithm for initial modeling of the amplifier.

Neural network	MLP
Training Algorithm	GA
Input Layer Neurons	4
Hidden Layer Neurons	7-7
Output Layer Neurons	6
Number of Iterations or Generations	100
Population Size	500
Activation Function	tansig

The mean squared error (MSE) of the initial proposed GA algorithm for the amplifier modeling versus number of iterations is depicted in Figure 6. As seen, the value of the mean squared error is decreasing as iterations number increase; however, this decrement rate will be reduced as number of iterations increases. The MSE equation which is used in this paper is defined in Equation (6):

$$\mathrm{MSE} = \frac{1}{N}\sum_{i=1}^{N}(Y_{\mathrm{Re}i} - Y_{\mathrm{Pr}i})^2 \tag{6}$$

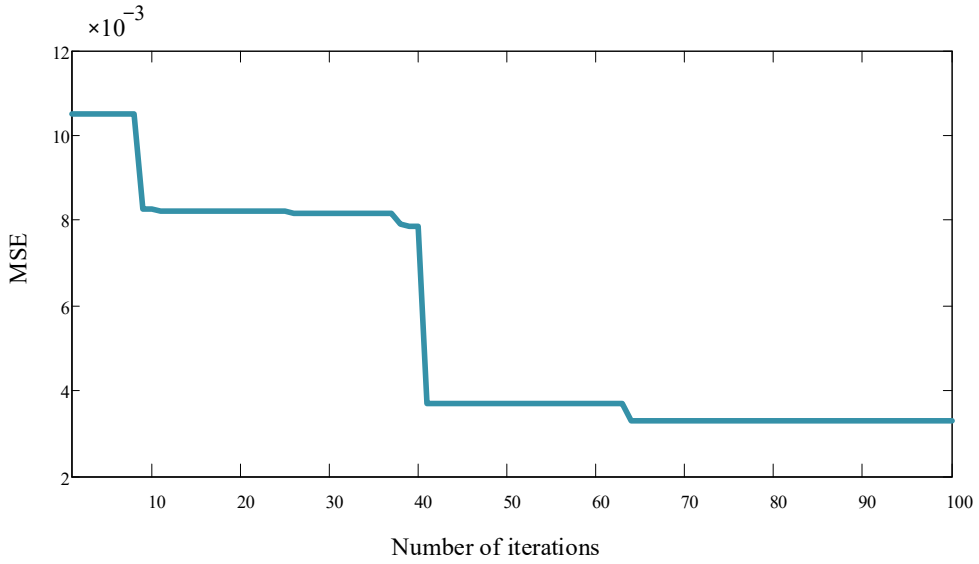

Figure 6. MSE of the initial proposed GA versus number of iterations.

3.2.3. MLP-PSO Neural Optimization Network

The PSO algorithm, which was developed in 1995, is based on the behavior of social mechanism, for instance, a flock of birds [53]. The PSO method is an evolutionary method, similar to the genetic algorithm. In the PSO algorithm, each particle is determined dependent upon its velocity and position. Experiences of neighboring particles affect the behavior of each particle. Other particles follow the best performance particle to find its solution [54]. The parameters of the PSO algorithm, applied in the presented ANN network, are swarm particles number of 500 and 100 iterations. The specifications of the PSO algorithm for initial modeling of the amplifier are listed in Table 3. The mean squared error of the initial proposed PSO algorithm for the amplifier modeling versus number of iterations is depicted in Figure 7. As seen, the value of MSE is exponentially decreasing as the number of iterations increases.

Table 3. Specifications of the PSO algorithm for initial modeling of the amplifier.

Neural network	MLP
Training algorithm	PSO
Input layer neurons	4
Hidden layer neurons	7-7
Output layer neurons	6
Number of iterations or generations	100
Population Size	500
Activation function	Tansig
Cognition Coefficient	2
Social Coefficient	2

Table 4. Summary of the results of the initial hybrid ANN-optimization networks.

Error	ANN-ICA Test	ANN-ICA Train	ANN-GA Test	ANN-GA Train	ANN-PSO Test	ANN-PSO Train
MAE, R (Ω)	8.20	8.97	15.68	10.97	7.33	3.34
RMSE, R (Ω)	15.31	11.69	21.47	16.36	11.72	4.50
MAE, L (uH)	11.04	10.63	21.38	16.70	7.95	6.49
RMSE, L (uH)	12.88	14.46	33.55	20.47	9.55	7.97
MAE, C (nF)	0.25	0.22	0.03	0.02	0.35	0.18
RMSE, C (nF)	0.36	0.31	0.04	0.02	0.56	0.25
MAE, C_{sh} (nF)	0.22	0.28	0.49	0.33	0.34	0.24
RMSE, C_{sh} (nF)	0.28	0.36	0.67	0.40	0.49	0.37
MAE, v_o (V)	1.92	2.37	3.74	3.19	0.58	0.45
RMSE, v_o (V)	2.44	2.83	4.41	3.96	0.90	0.67
MAE, v_s (V)	8.92	6.93	12.60	9.32	1.12	1.15
RMSE, v_s (V)	11.67	8.96	16.52	11.73	1.43	1.50

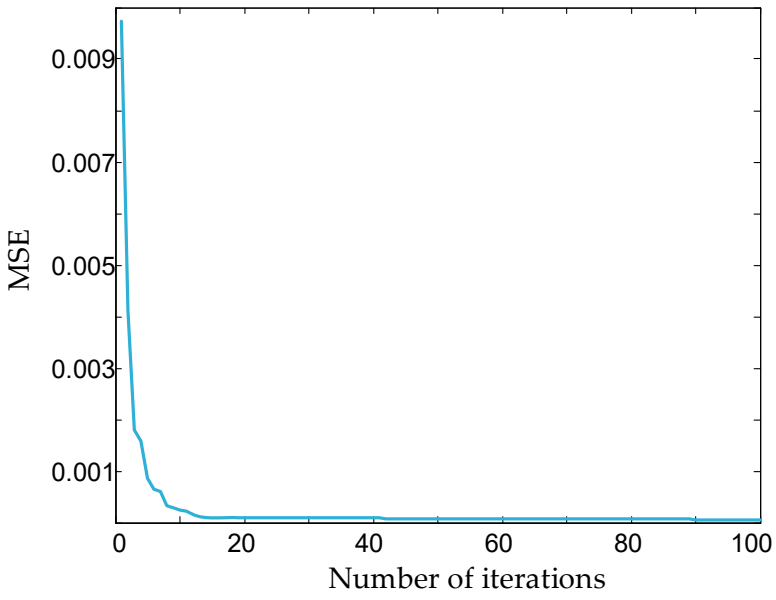

Figure 7. MSE of the initial proposed PSO algorithm versus the number of iterations.

4. Results and Discussion

As mentioned, low number of iterations is selected for hybrid ANN-optimization networks according to initial evaluation. The results summary of the initial hybrid ANN-optimization networks is given in Table 4. As seen, the ANN-PSO optimization network has the best results, compared to the other networks. Thus, the ANN-PSO optimization network is selected for the final modeling of the class-E amplifier.

Subsequently, the ANN-PSO optimization network, which has the best results compared to the other networks, is selected for the final modeling of the class-E amplifier.

Hence, swarm particles of 500 and iterations of 1000 are considered for the final proposed ANN–PSO network. The result summary of the final proposed ANN–PSO network is given in Table 5.

Table 5. Summary of the results of the final proposed ANN–PSO network.

Error	ANN-PSO Test	ANN-PSO Train	ANN-PSO Test (Normalized Data)	ANN-PSO Train (Normalized Data)
MAE, R (Ω)	2.39	1.91	0.0042	0.0034
RMSE, R (Ω)	3.40	2.38	0.0060	0.0042
MAE, L (uH)	3.63	2.43	0.0040	0.0027
RMSE, L (uH)	4.45	3.10	0.0049	0.0034
MAE, C (nF)	0.1	0.11	0.0252	0.0290
RMSE, C (nF)	0.12	0.17	0.0310	0.0444
MAE, C_{sh} (nF)	0.11	0.14	0.0220	0.0283
RMSE, C_{sh} (nF)	0.13	0.21	0.0268	0.0421
MAE, v_o (V)	0.19	0.11	0.0021	0.0012
RMSE, v_o (V)	0.27	0.15	0.0028	0.0016
MAE, v_s (V)	0.65	0.49	0.0020	0.0015
RMSE, v_s (V)	0.86	0.66	0.0027	0.0021
Mean Value–MAE	1.17	0.86	0.0099	0.0110
Mean Value–RMSE	1.53	1.11	0.0124	0.0163

As seen in the Table 5, the proposed model has precisely predicted the output values. There are six circuit elements which are considered as the output of the proposed model. Therefore, typically, the predicted results of the output resistor of the circuit are reported. The predicted and real values of the final proposed ANN–PSO network algorithm for the output resistor element are shown in Figure 8. In this figure, real values of the resistor, which are extracted by the analyses, are shown as the real resistor values with solid line, whereas the predicted values of resistor by the proposed ANN are shown with circles. According to this figure, the model could predict the power amplifier circuit parameter, precisely.

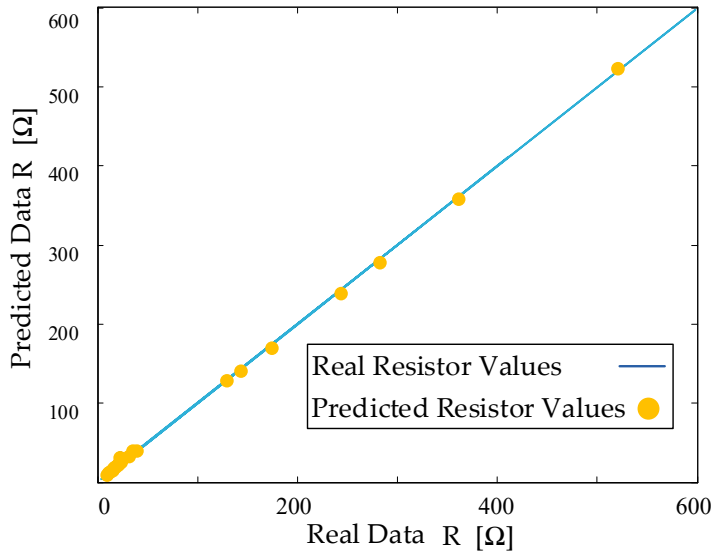

(**a**)

Figure 8. *Cont.*

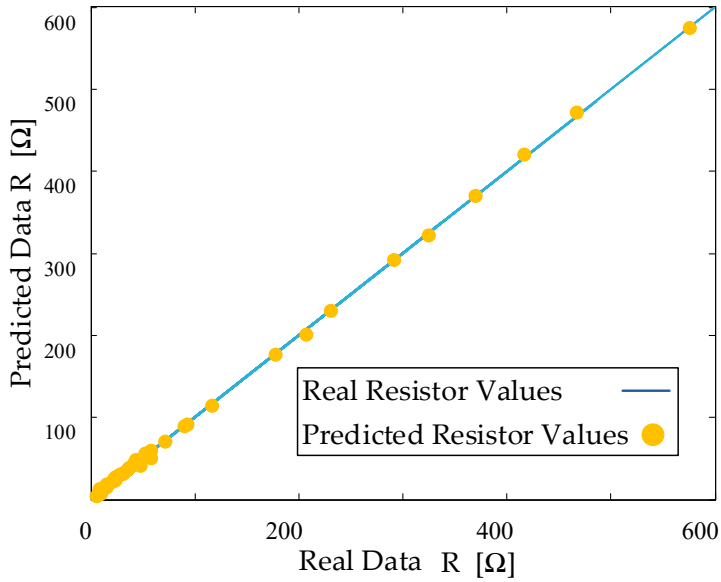

(**b**)

Figure 8. Real and predicted circuit output resistor values for (**a**) test and (**b**) train data of the final proposed ANN–PSO network.

The MSE of the final proposed ANN–PSO network for the amplifier modeling versus number of iterations is depicted in Figure 9. As seen, good MSE has been obtained at the end of the iterations. The MSE formula used in this paper is defined in Equation (6).

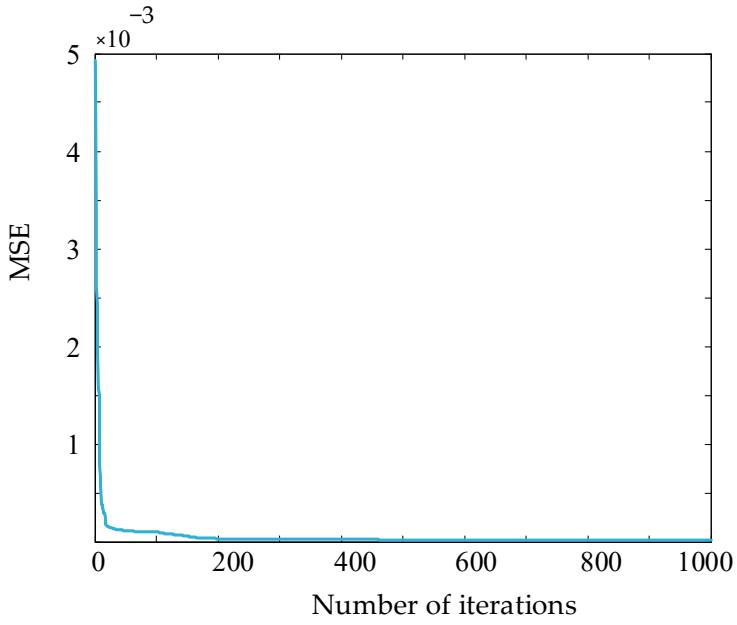

Figure 9. MSE of the final proposed ANN–PSO network versus number of iterations for the output resistor.

The predicted and real circuit output resistor values of the proposed final ANN–PSO network algorithm versus the number of samples are shown in Figure 10. As seen in this figure, out of 100 sample data, 80 samples are considered to train the model and the other 20 samples are selected for the test procedure of the model.

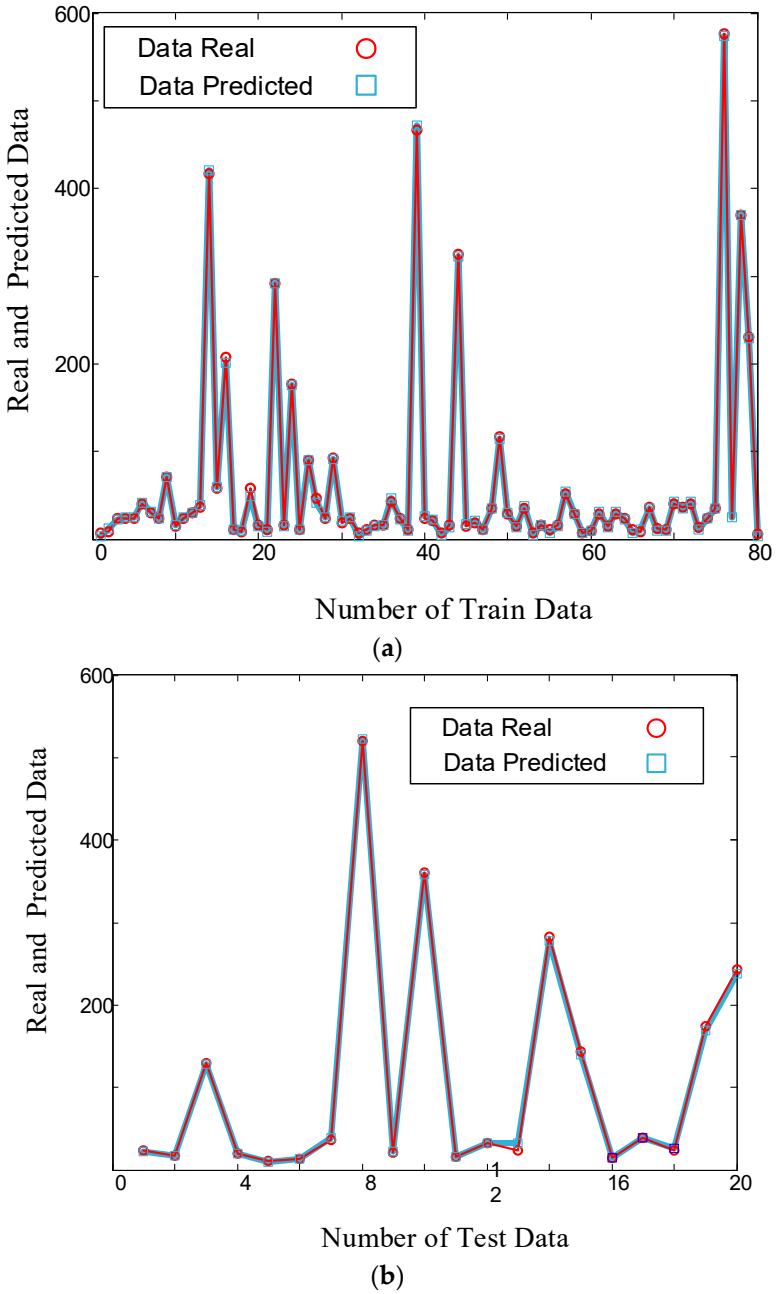

Figure 10. Real and predicted circuit output resistor values for (**a**) train and (**b**) test data of the final proposed ANN–PSO network versus number of samples.

4.1. The Proposed Model Comparison

The proposed class-E ANN model with its selected model parameters, is presented for the first time in this work. However, by using the average of the output parameters errors, the presented model can be compared with the similar ANN models. A complete report of the proposed model errors is shown in Table 5. A comparison between the test and train error results of the proposed model is listed in Table 6. According to the reported results in Table 6, the proposed class-E PA model has precise results.

Table 6. A comparison between the test and train error results of the proposed model.

Errors	Proposed Model Training	Proposed Model Testing
MAE	0.0110	0.0099
RMSE	0.0163	0.0124

4.2. Design Examples

To validate the proposed model, a design example of class-E PA is presented at 1 MHz. A comparison between the final proposed ANN–PSO model and analyses results of the presented design example is listed in Table 7. The "Analyses Result Values" column in Table 7 is calculated by solving the typical equations for conventional class-E amplifier [14]. These equations are solved using MATLAB software. Moreover, the "Model Result Values" column in Table 7 shows the predicted values by the proposed ANN–PSO model. When parasitic elements of the amplifier have been considered in the circuit, equations will become more complicated, but the proposed model could easily predict the circuit parameters.

Table 7. Comparison between the final model and analysis results of the presented design example at 1 MHz.

Input Parameters	Considered Values	Output Parameters	Analyses Result Values	Model Result Values	Relative Error
V_{DC} (V)	20	R (Ω)	23.07	25.07	0.086
P_o (W)	10	L (uH)	36.72	39.64	0.079
f (MHz)	1	C (pF)	779.6	802.0	0.028
Q	10	C_{ex} (pF)	1186.5	1225.5	0.032
		v_o (V)	21.48	21.43	0.002
		v_{sm} (V)	71.24	70.87	0.005

The presented design example of a class-E amplifier is simulated once with the circuit elements obtained by solving amplifier equations. Additionally, the presented design example is simulated again using circuit elements extracted from the final proposed ANN–PSO model. A comparison between class-E simulation results using extracted circuit parameters from analyses and the proposed model are illustrated in Figure 11, which shows good accuracy of the model. The simulation is performed using Orcad Capture 9.2 software included in PSpice programs. The calculated drain efficiencies for the designed class-E amplifiers have been obtained equal to 95.5% and 91.2% by using analyses data and predicted data by proposed ANN, respectively. Additionally, the output power capabilities have been calculated as 0.1 and 0.09 for the designed amplifier by using analyses data and predicted data, respectively.

Another design example of class-E PA is presented at 1.8 MHz to show the effects of input frequency variation on the accuracy of the model. A comparison between the final proposed ANN–PSO model and analyses results of the presented design example at 1.8 MHz is listed in Table 8. According to this table, the proposed model could predict the circuit elements at different frequencies precisely.

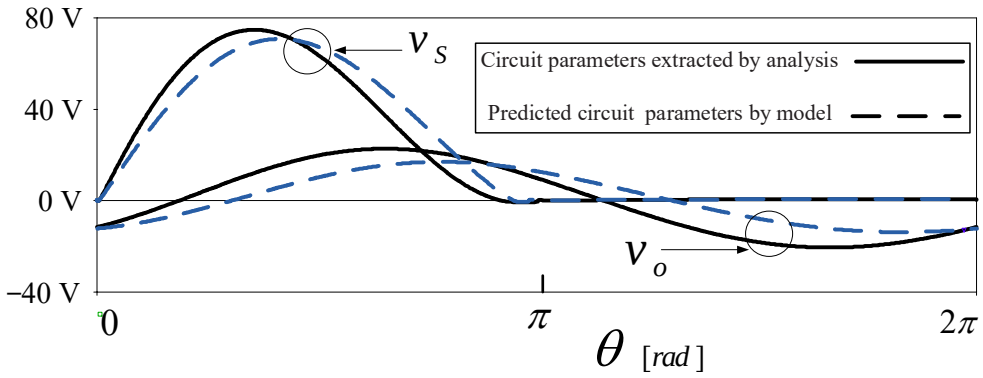

Figure 11. Class-E circuits simulation using extracted circuit parameters from analyses (solid line) and the proposed model (dashed line).

Table 8. A comparison between the final model and analysis results of the presented design example at 1.8 MHz.

Input Parameters	Considered Values	Output Parameters	Analyses Result Values	Model Result Values	Relative Error
V_{DC} (V)	20	R (Ω)	23	24.3	0.057
P_o (W)	10	L (uH)	20.4	18.7	0.083
f (MHz)	1.8	C (pF)	433.2	484.6	0.118
Q	10	C_{ex} (pF)	623.6	518.8	0.168
		v_o (V)	21.4	21.3	0.004
		v_{sm} (V)	71.2	71.3	0.001

4.3. Result Comparison

In this section, a comparison between the performance of the proposed algorithm and the other researches has been performed, which is listed in Table 9. As can be seen in Table 9, the ANN method is used in [37] for modeling of the amplifier and predict output parameter of the amplifier. Additionally, the ANN method is used in [43] for predicting load resistance and mutual inductance parameters in the WPT system. In [55], a feedforward neural network is presented for automatic impedance matching in WPT system. The effects of uncertain parameters in WPT system is predicted in [56] using partial least squares (PLS) regression method. Finally, ANN-PSO method, which is presented in this paper has the best results, while the proposed method can predict the design parameter of the amplifier for WPT applications.

Table 9. A comparison between the performance of proposed algorithm and other research papers.

Ref	Proposed Method	Design Parameter Prediction	Accuracy-Error Type
[37]	ANN	No	0.0311-MAE
[43]	ANN	No	0.0740-MRE 0.0293-MRE
[55]	ANN	No	0.5-RMSE
[56]	PLS regression	No	0.535-RMSE
This Work	ANN + PSO	Yes	0.0099-MAE 0.0124-RMSE

5. Conclusions

In this paper, a class-E PA model was presented using the hybrid artificial neural network and optimization algorithms for wireless power transfer (WPT) applications, to

be used in biomedical or internet of things (IoT) devices. By using the proposed model, the circuit elements of the amplifier can be easily predicted. Therefore, a class-E amplifier can be designed with desirable parameters, such as output power, DC voltage, and quality factor, at any frequency using the proposed model. Two operating frequencies of 1 MHz and 1.8 MHz are considered for two design examples, in which the presented model has predicted the circuit elements accurately. The MAE of better than 0.011 and MRE of better than 0.016 have been achieved in the proposed model. Moreover, the best- and worst-case related errors of 0.001 and 0.168 have been obtained, respectively, in both design examples. A comparison between the simulation results based on the analyses and the simulation results based on the proposed ANN model shows good agreement. The proposed model is valid for the presented circuit and the modeling procedure can be applied to any amplifier circuit, which can simplify the RF circuit modeling process. The other advantage is that the presented modeling does not need complicated equations, especially when parasitic and nonlinear elements are considered in the circuit.

Author Contributions: S.R. (Sobhan Roshani), S.I.Y. and S.R. (Saeed Roshani); methodology, S.R. (Sobhan Roshani), Y.S.M., B.M.A. and S.R. (Saeed Roshani); software, M.A.C., M.J. and S.R. (Saeed Roshani); validation, M.J. and G.K.I.; formal analysis, S.I.Y. and S.R. (Saeed Roshani); investigation, S.R. (Saeed Roshani); resources, S.R. (Sobhan Roshani); writing—original draft preparation, S.R. (Sobhan Roshani) and S.R. (Saeed Roshani); writing—review and editing, B.M.A., M.J., M.A.C., G.K.I., Y.S.M. and S.I.Y. All authors have read and agreed to the published version of the manuscript.

Funding: This research received no external funding.

Data Availability Statement: All the material conducted in the study is mentioned in article.

Conflicts of Interest: The authors declare no conflict of interest.

References

1. Tesla, N. Electrical Energy. U.S. Patent 1,119,732, 1 December 1914.
2. Liu, H.; Shao, Q.; Fang, X. Modeling and optimization of class-E amplifier at subnominal condition in a wireless power transfer system for biomedical implants. *IEEE Trans. Biomed. Circuits Syst.* **2016**, *11*, 35–43. [CrossRef] [PubMed]
3. Rana, M.M.; Xiang, W.; Wang, E.; Li, X.; Choi, B.J. Internet of Things infrastructure for wireless power transfer systems. *IEEE Access* **2018**, *6*, 19295–19303. [CrossRef]
4. Li, S.; Mi, C.C. Wireless power transfer for electric vehicle applications. *IEEE J. Emerg. Sel. Top. Power Electron.* **2014**, *3*, 4–17.
5. Xie, L.; Shi, Y.; Hou, Y.T.; Lou, A. Wireless power transfer and applications to sensor networks. *IEEE Wirel. Commun.* **2013**, *20*, 140–145.
6. Zhang, Z.; Pang, H.; Georgiadis, A.; Cecati, C. Wireless power transfer—An overview. *IEEE Trans. Ind. Electron.* **2018**, *66*, 1044–1058. [CrossRef]
7. Xue, R.-F.; Cheng, K.-W.; Je, M. High-efficiency wireless power transfer for biomedical implants by optimal resonant load transformation. *IEEE Trans. Circuits Syst. I Regul. Pap.* **2012**, *60*, 867–874. [CrossRef]
8. Hayati, M.; Roshani, S.; Kazimierczuk, M.K.; Sekiya, H. A class-E power amplifier design considering MOSFET nonlinear drain-to-source and nonlinear gate-to-drain capacitances at any grading coefficient. *IEEE Trans. Power Electron.* **2015**, *31*, 7770–7779. [CrossRef]
9. Hayati, M.; Roshani, S.; Kazimierczuk, M.K.; Sekiya, H. Analysis and design of class E power amplifier considering MOSFET parasitic input and output capacitances. *IET Circuits Devices Syst.* **2016**, *10*, 433–440. [CrossRef]
10. Jamshidi, M.B.; Roshani, S.; Talla, J.; Sharifi-Atashgah, M.S.; Roshani, S.; Peroutka, Z. Cloud-based Machine Learning Techniques Implemented by Microsoft Azure for Designing Power Amplifiers. In Proceedings of the 2021 IEEE 12th Annual Ubiquitous Computing, Electronics & Mobile Communication Conference (UEMCON), New York, NY, USA, 1–4 December 2021; pp. 41–44.
11. Tirado-Mendez, A.; Jardon-Aguilar, H.; Flores-Leal, R.; Andrade-Gonzalez, E.; Reyes-Ayala, M. Low-harmonic distortion in single-ended and push-pull class E power amplifier by using slotted microstrip lines. *AEU-Int. J. Electron. Commun.* **2010**, *64*, 66–74. [CrossRef]
12. Sharma, T.; Aflaki, P.; Helaoui, M.; Ghannouchi, F.M. Broadband GaN class-E power amplifier for load modulated delta sigma and 5G transmitter applications. *IEEE Access* **2018**, *6*, 4709–4719. [CrossRef]
13. Sokal, N.O.; Sokal, A.D. Class EA new class of high-efficiency tuned single-ended switching power amplifiers. *IEEE J. Solid-State Circuits* **1975**, *10*, 168–176. [CrossRef]
14. Kazimierczuk, M.K. *RF Power Amplifiers*; John Wiley & Sons: Hoboken, NJ, USA, 2014.
15. Wei, X.; Sekiya, H.; Kuroiwa, S.; Suetsugu, T.; Kazimierczuk, M.K. Design of class-E amplifier with MOSFET linear gate-to-drain and nonlinear drain-to-source capacitances. *IEEE Trans. Circuits Syst. I Regul. Pap.* **2011**, *58*, 2556–2565. [CrossRef]

16. Suetsugu, T.; Kazimierczuk, M.K. Design procedure of class-E amplifier for off-nominal operation at 50% duty ratio. *IEEE Trans. Circuits Syst. I Regul. Pap.* **2006**, *53*, 1468–1476. [CrossRef]
17. Mury, T.; Fusco, V.F. Inverse class-E amplifier with transmission-line harmonic suppression. *IEEE Trans. Circuits Syst. I Regul. Pap.* **2007**, *54*, 1555–1561. [CrossRef]
18. Chokkalingam, B.; Padmanaban, S.; Leonowicz, Z.M. Class E power amplifier design and optimization for the capacitive coupled wireless power transfer system in biomedical implants. *Energies* **2017**, *10*, 1409.
19. Bertoni, N.; Frattini, G.; Massolini, R.G.; Pareschi, F.; Rovatti, R.; Setti, G. An analytical approach for the design of class-E resonant DC–DC converters. *IEEE Trans. Power Electron.* **2016**, *31*, 7701–7713. [CrossRef]
20. Garcia, J.A.; Popović, Z. Class-E rectifiers and power converters: The operation of the class-E topology as a power amplifier and a rectifier with very high conversion efficiencies. *IEEE Microw. Mag.* **2018**, *19*, 67–78. [CrossRef]
21. Srimuang, P.; Puangngernmak, N.; Chalermwisutkul, S. 13.56 MHz class E power amplifier with 94.6% efficiency and 31 watts output power for RF heating applications. In Proceedings of the 2014 11th International Conference on Electrical Engineering/Electronics, Computer, Telecommunications and Information Technology (ECTI-CON), Nakhon Ratchasima, Thailand, 14–17 May 2014; pp. 1–5.
22. Dai, W.; Tang, W.; Cai, C.; Deng, L.; Zhang, X. Wireless power charger based on class E amplifier with the maximum power point load consideration. *Energies* **2018**, *11*, 2378. [CrossRef]
23. Sutor, A.; Heining, M.; Buchholz, R. A class-e amplifier for a loosely coupled inductive power transfer system with multiple receivers. *Energies* **2019**, *12*, 1165. [CrossRef]
24. Hashemi, M.; Zhou, L.; Shen, Y.; De Vreede, L.C. A highly linear wideband polar class-E CMOS digital Doherty power amplifier. *IEEE Trans. Microw. Theory Tech.* **2019**, *67*, 4232–4245. [CrossRef]
25. Barzgari, M.; Ghafari, A.; Nikpaik, A.; Medi, A. Even-harmonic class-E CMOS oscillator. *IEEE J. Solid-State Circuits* **2021**, *57*, 1594–1609. [CrossRef]
26. Parandin, F.; Karkhanehchi, M.M. Low size all optical XOR and NOT logic gates based on two-dimensional photonic crystals. *Majlesi J. Electr. Eng.* **2019**, *13*, 1–5.
27. Vahdati, A.; Parandin, F. Antenna patch design using a photonic crystal substrate at a frequency of 1.6 THz. *Wirel. Pers. Commun.* **2019**, *109*, 2213–2219. [CrossRef]
28. Karkhanehchi, M.M.; Parandin, F.; Zahedi, A. Design of an all optical half-adder based on 2D photonic crystals. *Photonic Netw. Commun.* **2017**, *33*, 159–165. [CrossRef]
29. Parandin, F. Ultra-compact terahertz all-optical logic comparator on GaAs photonic crystal platform. *Opt. Laser Technol.* **2021**, *144*, 107399. [CrossRef]
30. Planat, L.; Ranadive, A.; Dassonneville, R.; Martínez, J.P.; Léger, S.; Naud, C.; Buisson, O.; Hasch-Guichard, W.; Basko, D.M.; Roch, N. Photonic-crystal Josephson traveling-wave parametric amplifier. *Phys. Rev. X* **2020**, *10*, 021021. [CrossRef]
31. Kotb, A.; Zoiros, K.E.; Guo, C. Ultrafast performance of all-optical AND and OR logic operations at 160 Gb/s using photonic crystal semiconductor optical amplifier. *Opt. Laser Technol.* **2019**, *119*, 105611. [CrossRef]
32. Hayati, M.; Roshani, S.; Roshani, S.; Kazimierczuk, M.K.; Sekiya, H. Design of class E power amplifier with new structure and flat top switch voltage waveform. *IEEE Trans. Power Electron.* **2017**, *33*, 2571–2579. [CrossRef]
33. Roshani, G.H.; Roshani, S.; Nazemi, E.; Roshani, S. Online measuring density of oil products in annular regime of gas-liquid two phase flows. *Measurement* **2018**, *129*, 296–301. [CrossRef]
34. Chen, T.-C.; Taylan, O.; Alizadeh, S.M.; Yilmaz, M.T.; Nazemi, E.; Balubaid, M.; Roshani, G.H.; Karaboga, D. Investigation of Time-Domain Feature Selection and GMDH Neural Network Application for Determination of Volume Percentages in X-Ray-Based Two-Phase Flow Meters. *MAPAN* **2022**, 1–13. [CrossRef]
35. Roshani, M.; Sattari, M.A.; Ali, P.J.M.; Roshani, G.H.; Nazemi, B.; Corniani, E.; Nazemi, E. Application of GMDH neural network technique to improve measuring precision of a simplified photon attenuation based two-phase flowmeter. *Flow Meas. Instrum.* **2020**, *75*, 101804. [CrossRef]
36. Roshani, M.; Phan, G.; Roshani, G.H.; Hanus, R.; Nazemi, B.; Corniani, E.; Nazemi, E. Combination of X-ray tube and GMDH neural network as a nondestructive and potential technique for measuring characteristics of gas-oil–water three phase flows. *Measurement* **2021**, *168*, 108427. [CrossRef]
37. Zirak, A.R.; Roshani, S. Design and modeling of RF power amplifiers with radial basis function artificial neural networks. *Int. J. Adv. Comput. Sci. Appl.* **2016**, *7*, 227–231.
38. Mehrafrooz, A.; He, F.; Lalbakhsh, A. Introducing a Novel Model-Free Multivariable Adaptive Neural Network Controller for Square MIMO Systems. *Sensors* **2022**, *22*, 2089. [CrossRef]
39. Jamshidi, M.B.; Lalbakhsh, A.; Mohamadzade, B.; Siahkamari, H.; Mousavi, S.M.H. A novel neural-based approach for design of microstrip filters. *AEU-Int. J. Electron. Commun.* **2019**, *110*, 152847. [CrossRef]
40. Jamshidi, M.; Lalbakhsh, A.; Lotfi, S.; Siahkamari, H.; Mohamadzade, B.; Jalilian, J. A neuro-based approach to designing a Wilkinson power divider. *Int. J. RF Microw. Comput.-Aided Eng.* **2020**, *30*, e22091. [CrossRef]
41. Wang, M.; Feng, J.; Shi, Y.; Shen, M.; Jing, J. A Novel PSO-Based Transfer Efficiency Optimization Algorithm for Wireless Power Transfer. *Prog. Electromagn. Res. C* **2018**, *85*, 63–75. [CrossRef]

42. ELSayed, K.G.; Elessawy, N.A.; ElShenawy, A.K. Wireless power transfer system modelling based on neural network with adaptive filtering. In Proceedings of the 2015 International Conference on High Performance Computing & Simulation (HPCS), Amsterdam, The Netherlands, 20–24 July 2015; pp. 305–310.
43. He, L.; Zhao, S.; Wang, X.; Lee, C.-K. Artificial Neural Network-Based Parameter Identification Method for Wireless Power Transfer Systems. *Electronics* **2022**, *11*, 1415. [CrossRef]
44. Ali, A.; Mohd Yasin, M.N.; Jusoh, M.; Ahmad Hambali, N.A.M.; Abdul Rahim, S.R. Optimization of wireless power transfer using artificial neural network: A review. *Microw. Opt. Technol. Lett.* **2020**, *62*, 651–659. [CrossRef]
45. Karimi, H.; Yousefi, F. Application of artificial neural network–genetic algorithm (ANN–GA) to correlation of density in nanofluids. *Fluid Phase Equilibria* **2012**, *336*, 79–83. [CrossRef]
46. Toghyani, S.; Ahmadi, M.H.; Kasaeian, A.; Mohammadi, A.H. Artificial neural network, ANN-PSO and ANN-ICA for modelling the Stirling engine. *Int. J. Ambient. Energy* **2016**, *37*, 456–468. [CrossRef]
47. Atashpaz-Gargari, E.; Lucas, C. Imperialist competitive algorithm: An algorithm for optimization inspired by imperialistic competition. In Proceedings of the 2007 IEEE Congress on Evolutionary Computation, Singapore, 25–28 September 2007; pp. 4661–4667.
48. Mikaeil, R.; Haghshenas, S.S.; Haghshenas, S.S.; Ataei, M. Performance prediction of circular saw machine using imperialist competitive algorithm and fuzzy clustering technique. *Neural Comput. Appl.* **2018**, *29*, 283–292. [CrossRef]
49. Torquato, M.F.; Fernandes, M.A. High-performance parallel implementation of genetic algorithm on fpga. *Circuits Syst. Signal Process.* **2019**, *38*, 4014–4039. [CrossRef]
50. Szopos, E.; Neag, M.; Saracut, I.; Popescu, V.; Topa, M. Synthesis tool based on genetic algorithm for FIR filters with user-defined magnitude characteristics. *Circuits Syst. Signal Process.* **2016**, *35*, 253–279. [CrossRef]
51. Papadimitriou, A.; Bucher, M. Multi-objective low-noise amplifier optimization using analytical model and genetic computation. *Circuits Syst. Signal Process.* **2017**, *36*, 4963–4993. [CrossRef]
52. Goldberg David, E.; Henry, H. Genetic algorithms and machine learning. *Mach Learn* **1988**, *3*, 95–99. [CrossRef]
53. Kennedy, J. Particle swarm optimization. Encyclopedia of machine learning. *Springer* **2011**, *760*, 766.
54. De, B.P.; Kar, R.; Mandal, D.; Ghoshal, S.P. Particle swarm optimization with aging leader and challengers for optimal design of analog active filters. *Circuits Syst. Signal Process.* **2015**, *34*, 707–737. [CrossRef]
55. Jeong, S.; Lin, T.-H.; Tentzeris, M.M. A real-time range-adaptive impedance matching utilizing a machine learning strategy based on neural networks for wireless power transfer systems. *IEEE Trans. Microw. Theory Tech.* **2019**, *67*, 5340–5347. [CrossRef]
56. Larbi, M.; Trinchero, R.; Canavero, F.G.; Besnier, P.; Swaminathan, M. Analysis of parameter variability in an integrated wireless power transfer system via partial least-squares regression. *IEEE Trans. Compon. Packag. Manuf. Technol.* **2020**, *10*, 1795–1802. [CrossRef]